Safety studies on vacuum insulated liquid helium cryostats

IOP Conf. Series: Materials Science and Engineering **278** (2017) 012169 doi:10.1088/1757-899X/278/1/012169

Safety studies on vacuum insulated liquid helium cryostats

C Weber[1,2], A Henriques[4], C Zoller[3] and S Grohmann[1,2]

[1] Karlsruhe Institute of Technology (KIT), Institute for Technical Physics, Hermann-von-Helmholtz-Platz 1, 76344 Eggenstein-Leopoldshafen, Germany
[2] Karlsruhe Institute of Technology, Institute for Thermodynamics and Refrigeration, Kaiserstrasse 12, 76131 Karlsruhe, Germany
[3] Paul-Scherrer-Institute (PSI), WMHA/C46, 5232 Villigen PSI, Switzerland
[4] European Organization for Nuclear Research (CERN), CH-1211, Geneva 23, Switzerland

E-mail: christina.weber@kit.edu, carolin.heidt@psi.ch, andre.henriques@cern.ch, steffen.grohmann@kit.edu

Abstract. The loss of insulating vacuum is often considered as a reasonable foreseeable accident for the dimensioning of cryogenic safety relief devices (SRD). The cryogenic safety test facility PICARD was designed at KIT to investigate such events. In the course of first experiments, discharge instabilities of the spring loaded safety relief valve (SRV) occurred, the so-called *chattering* and *pumping* effects. These instabilities reduce the relief flow capacity, which leads to impermissible over-pressures in the system. The analysis of the process dynamics showed first indications for a smaller heat flux than the commonly assumed $4\,\mathrm{W/cm^2}$. This results in an oversized discharge area for the reduced relief flow rate, which corresponds to the lower heat flux.

This paper presents further experimental investigations on the venting of the insulating vacuum with atmospheric air under variation of the set pressure (p_{set}) of the SRV. Based on dynamic process analysis, the results are discussed with focus on effective heat fluxes and operating characteristics of the spring-loaded SRV.

Keywords: Safety, liquid helium, cryogenics

1. Introduction

The dimensioning of cryogenic SRD requires detailed knowledge on the process dynamics, especially on the pressure increase and the heat flux trend following reasonable foreseeable accidents such as venting of the insulating vacuum with atmospheric air. However, established standards [1,2] do not fully cover the conditions in liquid helium cryostats that are relevant for the protection against over-pressure. Instead of considering the process dynamics, sizing is often based on constant heat flux values [3–5] resulting in possibly oversized SRD.

First experiments at the cryogenic safety test facility PICARD[1] have been carried out in the course of an R&D collaboration between CERN and KIT. The results indicate a smaller heat flux value at the valves opening pressure than those commonly assumed and mentioned above. As a consequence of the oversized SRV, discharge instabilities as the so-called *chattering* and

[1] **P**ressure **I**ncrease in **C**ryostats and **A**nalysis of **S**afety **R**elief **D**evices.

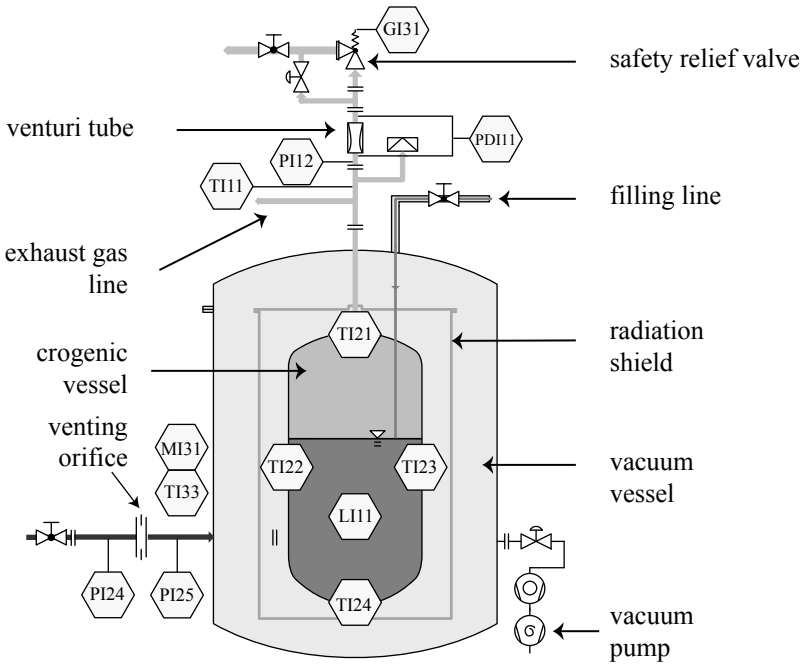

Figure 1. Simplified P&ID chart of the PICARD test facility. Updated from [7].

pumping occurred during these first experiments and impermissible over-pressures and reduced discharge flow rates were observed [6].

Based on these results, further experimental investigations have been conducted, where the insulating vacuum is vented with atmospheric air. Smaller dimensions of the SRV are used compared to previous measurements and the results are discussed with focus on the SRV behaviour, the pressure increase inside the cryogenic vessel and the dynamic trend of the heat flux.

The PICARD test set-up is shortly described in Section 2 of this paper. In order to introduce the theoretical framework, the general dimensioning of SRDs and the evaluation of the experimental data is explained in Section 3. The experimental results are presented in Section 4 and Section 5 closes the paper with a conclusion and an outlook.

2. Experimental set-up

The cryogenic safety test facility PICARD consits of a cryostat with a cryogenic volume of 100 L and has a maximum allowable pressure of 16 bar(g). More detailed information on the test facilty, the commissioning and first experimental results are published in [7, 8].

For further investigations, the PICARD instrumentation is extended by a proximity sensor (GI31) emitting pulsed laser light to measure the lift of SRVs during discharge with a calibration uncertainty of $\pm 0.5\,\%$. Furthermore, the differential pressure transmitter, which is needed to define the inflowing mass flow rate of air, is replaced by faster and more accurate relative pressure transmitters PI24 and PI25 with a calibration uncertainty of less than $\pm 0.05\,\%$. Hence, the measurement uncertainty of the calculated deposited heat flux is reduced. During experiments the data is sampled at a rate of 1 kHz. The P&ID of the test facility including all for this paper

relevant information is shown in Figure 1, with TI indicating a temperature sensor[2], PI a pressure transmitter, MI measures the humidity of air and GI the lift of the SRV.

Safety experiments at PICARD are initiated by venting the insulating vacuum with atmospheric air. The freezing of the humid air on the cold outer surface of the cryogenic vessel causes a heat flux which is transferred to the helium and thus, increases pressure and temperature inside the cryogenic vessel. When reaching the set pressure, the cold fluid is released through the installed SRV. A detailed description of the venting process is given in [6].

For the presented experiments, a spring loaded SRV of *Type 459* from *LESER GmbH* with a narrowest cross section of 240.5 mm^2 is used.

3. Theoretical framework

This section gives a short overview of the equations required for the general dimensioning of SRDs and introduces the calculation of the deposited heat flux and the discharge mass flow rate based on experimental results.

3.1. General dimensioning of safety relief devices

The required discharge area A_0 of SRDs is calculated according to common standards [1,2] as

$$A_0 = \frac{\dot{M}_{\mathrm{Out}}}{\Psi \cdot K_{\mathrm{dr}} \cdot \sqrt{2 \cdot \frac{p_0}{v_0}}} \,. \tag{1}$$

$\dot{M}_{\mathrm{Out}}$ is the discharge mass flow rate, Ψ the discharge function, K_{dr} the certified discharge coefficient, p_0 the relieving pressure and v_0 the specific volume at relieving conditions.

p_0 follows as a result of the safety concept of the pressure equipment [10]. For SRVs, this is the pressure at which the valve reaches full lift, whereas at the set pressure the SRV commences to open. $\dot{M}_{\mathrm{Out}}$ as a function of the deposited heat flux $\dot{q}_{\mathrm{Dep}}$ and v_0 are determined as explained in [11]. For supercritical fluid state that often occur for helium due to its low critical pressure the mass flow rate determination is based on the calculation of [12]. Constant heat flux values are given in literature [3–5]. The calculation of Ψ depending on the back-pressure and isentropic exponent is further explained in the standards. The K_{dr} is given by

$$K_{\mathrm{dr}} = 0.9 \, \frac{\dot{M}_{\mathrm{Out,measured}}}{\dot{M}_{\mathrm{Out,idealorifice}}} \,, \tag{2}$$

$\dot{M}_{\mathrm{Out,measured}}$ is the actual and $\dot{M}_{\mathrm{Out,idealorifice}}$ the theoretical discharge mass flow rate, hence, correcting the deviation of the SRV from an ideal nozzle. Manufacturer provide only measured values for gaseous and liquid flow and air respectively water as relieving fluid. In case of two-phase flow, various correlations depending on thermodynamical or fluiddynamical properties as well as the single phase K_{dr} values are available in literature [13–16] but not validated for helium.

3.2. Heat flux evaluation

The heat flux $\dot{q}_{\mathrm{Dep}}$ transferred to the helium due to freezing of humid air on the outer surface of the cryogenic vessel is calculated as

$$\dot{q}_{\mathrm{Dep}} = \frac{\dot{M}_{\mathrm{Dep}}}{A_{\mathrm{Cr}}} \cdot \Delta h_{\mathrm{Vent}} \,. \tag{3}$$

[2] TVO-sensors, which are carbon ceramic temperature sensors produced in Russia, are used for the measurement of cryogenic temperatures [9].

$\dot{M}_{\mathrm{Dep}}$ is the depositing mass flow rate, A_{Cr} the outer surface of the cryogenic vessel and Δh_{vent} the enthalpy difference of the venting fluid, i.e. the fluid flowing into the insulating vacuum. A detailed derivation of the heat flux calculation is given in [6]. While Δh_{vent} is calculated for pure nitrogen fluid data in [6], humid air (Δh_{Air}) is used in this work, assuming an ideal mixture of nitrogen, oxygen, argon and water. The humidity of the inflowing air is measured next to the venting line with a combined hygrometer (MI31) and temperature sensor (TI33) [8] and directly implemented in the enthalpy calculation. Δh_{Air} is calculated, taking into account the sensible and latent heat of all components from ambient (TI33 = T_{Amb}) to the measured cryogenic average wall temperature T_{Wall}. T_{Wall} is defined as an arithmetic average of the four installed wall temperature sensors TI21-TI24. The results were compared to REFPROP [17–21] real fluid data yielding a maximum deviation of 0.2 % in enthalpy. Hence, the ideal mixture assumption is justified. The difference of the humid air calculation compared to pure nitrogen is up to about +10 % depending on the humidity of air.

3.3. Discharge mass flow rate evaluation

The discharge mass flow rate is measured with a Venturi tube according to [22] as

$$\dot{M}_{\mathrm{Out}} = \frac{C_{\mathrm{Venturi}}}{\sqrt{1-\beta_{\mathrm{Venturi}}^4}} \cdot \epsilon_{\mathrm{Venturi}} \cdot \frac{\pi}{4} \cdot d_{\mathrm{Venturi}} \cdot \sqrt{2 \cdot \mathrm{PDI11} \cdot \rho_{\mathrm{Cr}}\left(\mathrm{PI12}, \mathrm{TI11}\right)}\,, \tag{4}$$

with the density of helium ρ_{Cr}, the throat diameter d_{Venturi}, the diameter ratio β_{Venturi}, the flow coefficient C_{Venturi} for classical Venturi tubes and the expansion coefficient $\epsilon_{\mathrm{Venturi}}$.

4. Experimental results

Table 1 gives an overview on two experiments, Exp. 1 and Exp. 2, discussed in this paper. For the first experiment the SRV has been designed applying (1) using a constant heat flux of 4 W/cm^2 [3]. The actual nominal valve size DN25 with a throat diameter of 17.5 mm yields a slight over-sizing of about 6 % compared to the theoretical dimensioning of the SRV according to Subsection 3.1. Figure 2 summarizes the results of the first experiment, with a) illustrating the time-dependent helium pressure profile (black) and the course of the lift of the SRV (gray) b) showing the discharge mass flow rate and c) the heat flux up to 80 s after venting. The lighter gray zones display the measurement uncertainties calculated according to [23]. When the insulating vacuum is vented, the pressure increases up to the set pressure. Ideally, the SRV opens and reaches full lift within the standardized 10 % [24] and within 5 % for full-lift SRVs as denoted by the manufacturer. Due to shrinking of the valve's stem as a consequence of cooling a zero point drift of the valve lift measurement is visible in Figure 2a). The lift measurement also shows *chattering* within 15 s after the first opening, yielding over-pressures (p_{max}) of about 13 % of the set pressure. *Pumping* occurs between 50 and 75 s when the maximum discharge mass flow rate is not reached any more due to a little rest of gas remaining in the vessel after the first opening. Compared to the calculated value, only about 50 % of the discharge mass flow rate is actually measured. Hence, *chattering* occurs due to a significantly oversized SRV.

Table 1. Overview of the sizing parameters compared to experimental results.

Exp.	p_{set} / bar(g)	A / mm^2		$\dot{q}_{\mathrm{Dep}}$ / W·cm^{-2}		$\dot{M}_{\mathrm{Out}}$ / kg·s^{-1}	
		Sizing	Experiment	Sizing	Experiment	Sizing	Experiment
1	8.0	227.0	240.5	4.0	1.8	1.2	0.58
2	4.5	208.7	240.5	1.8	2.0	0.9	0.45

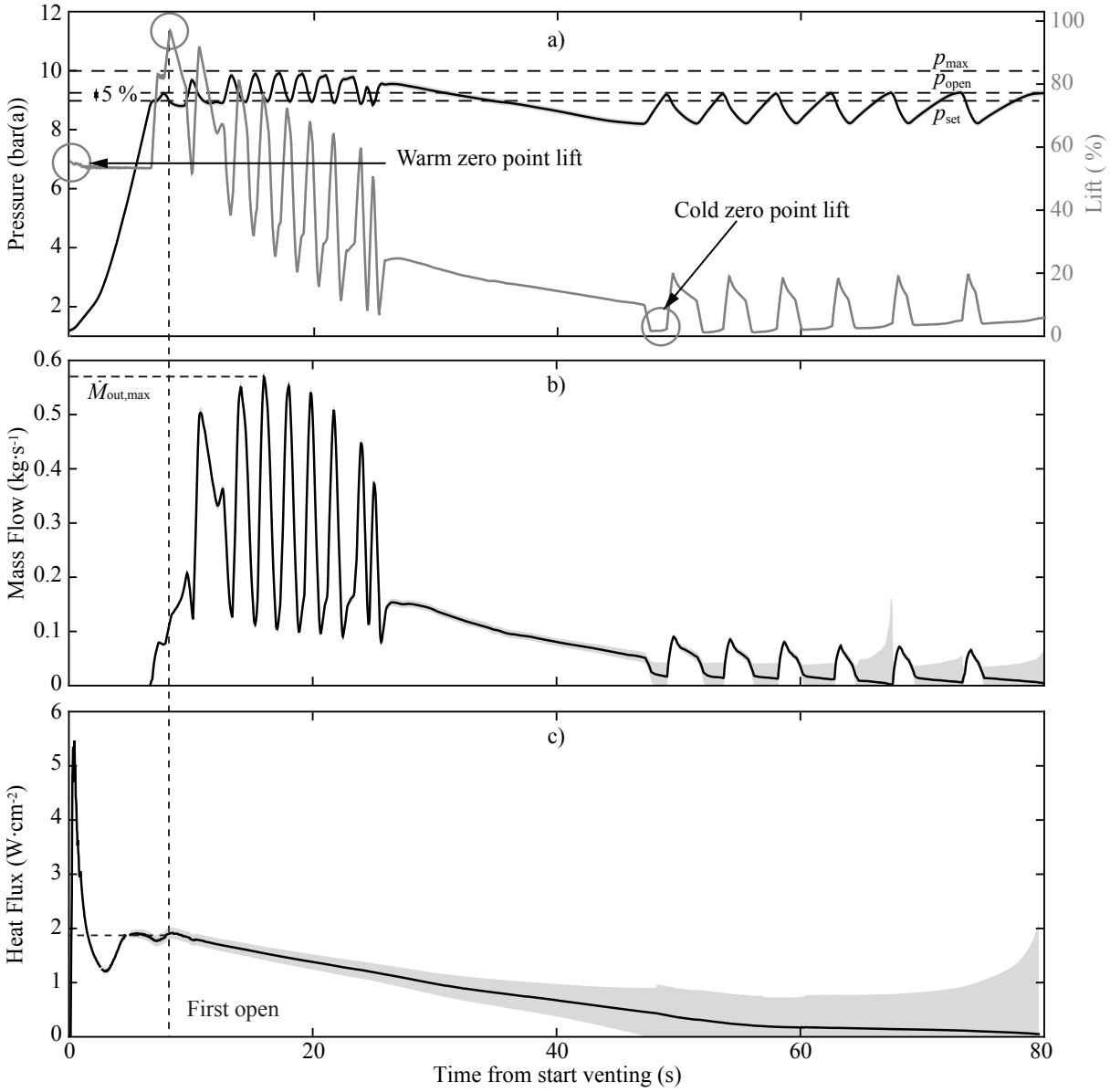

Figure 2. Results of Exp. 1. a) Pressure increase (PI12) and lift trend (GI31), b) profile of the discharge mass flow rate and c) profile of the heat flux after venting of the insulating vacuum with atmospheric air.

The time-dependent heat flux profile determined by (3) is shown in Figure 2c). Directly after the start of the experiment, high temperature differences between the inflowing air and the wall result in a maximum heat flux of about $5\,\mathrm{W/cm^2}$. This peak value is not relevant for the valve sizing, as it decreases strongly due to the insulating frost layer formation on the vessel surface. At the time of the opening of the SRV the heat flux reaches a value of $1.8 \pm 0.1\,\mathrm{W/cm^2}$, i.e. 55 % lower than the $4\,\mathrm{W/cm^2}$ assumed for sizing. The independent measurements of the discharge mass flow rate and the deposited heat flux agreed well within a deviation of 5 %.

The results of Experiment 1 also confirm the conclusions in [6], where oversizing of the SRV by using established maximum heat flux values from literature [3–5] causes unstable operation

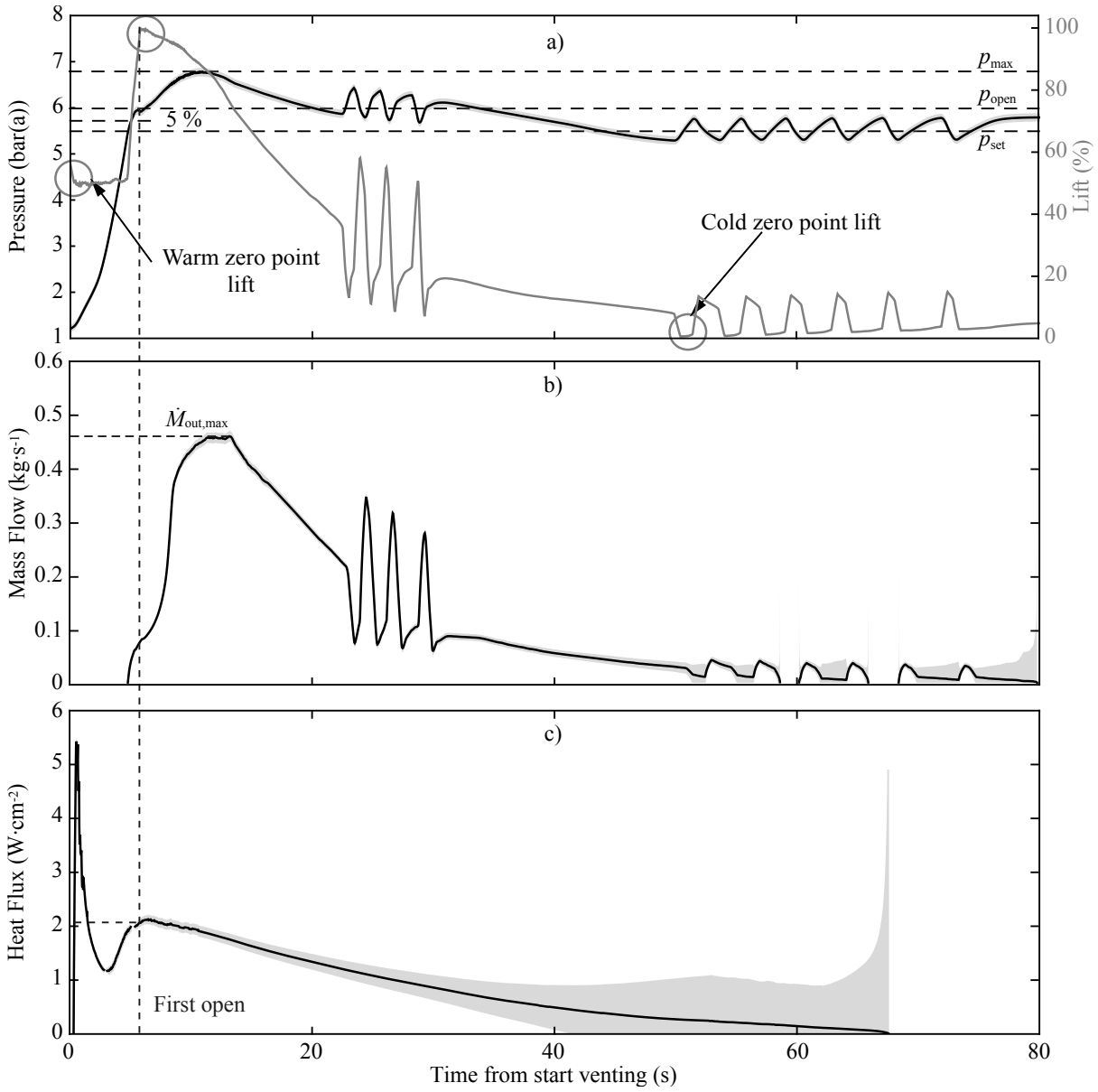

Figure 3. Results of Exp. 2. a) Pressure increase (PI12) and lift trend (GI31), b) profile of the discharge mass flow rate and c) profile of the heat flux after venting of the insulating vacuum with atmospheric air.

of the SRV which has a larger discharge area of 415 mm^2 and lower set pressures. Based on these results and the measured heat flux value of 1.8 W/cm^2 in the first experiment, the sizing of the SRV has been adapted in the second experiment. Following (1) a lower heat flux provides a lower discharge mass flow rate yielding a lower set pressure for the same dimensions of the SRV. Therefore, the set pressure in the second experiment is adjusted to 4.5 bar(g). Relevant sizing parameters compared to the experimental results are also listed in Table 1. For this conditions the SRV is again slightly oversized by 13 %.

Figure 3 summarizes the results of the second experiment, a) showing again the pressure and lift trend b) the discharge mass flow rate and c) depicts the heat flux profile. First of all, a

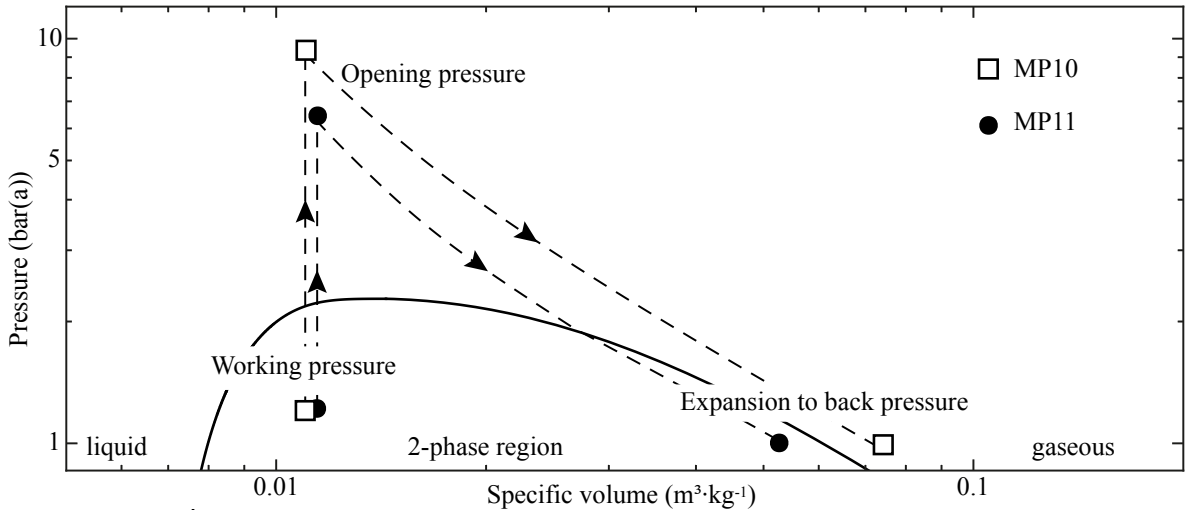

Figure 4. Helium p-v phase diagram including the isenthalpic relieving process paths of both experiments. The consideration of heat input during expansion, on one hand, yields flatter curves. Fluid acceleration up to critical flow, on the other hand, implies steeper curves.

stable operation of the SRV is achieved after the first opening. Only a few pumping steps occur when the SRV opens for a second time and again the maximum mass flow rate is not reached any more. Secondly, the SRV does not reach full lift within the 5 % above set pressure and significant over-pressures up to 27 % occur. The heat flux calculation applying again (3) yields a value of $2.1 \pm 0.07\,\mathrm{W/cm^2}$. Due to the lower set pressure in Exp. 2, the SRV commences to open earlier after venting, which results in a slightly higher heat flux value compared to Exp. 1. The measured discharge mass flow rate of 0.45 kg/s, however, is again only 50 % of the mass flow rate calculated with the heat flux of $1.8\,\mathrm{W/cm^2}$. Although a realistic heat flux is used for sizing now, the discharge area is too small to release the required mass flow rate yielding thus, the impermissible over-pressures.

Considering (1) the influence of K_{dr} must be discussed further. If the K_{dr} value is defined too high due to fluid state influences, the area is undersized, although the mass flow calculation is carried out based on realistic assumptions. Figure 4 shows the p-v phase diagram of helium including the relieving process paths of both experiments. Before venting of the insulating vacuum with atmospheric air, helium's working points are in the two-phase region defined by the filling level. When the insulating vacuum is vented, an isochoric pressure rising occurs in the closed system. Reaching the supercritical set pressure, helium expands through the open SRV to the back pressure. Depending on the filling level and the set pressure, the state point after the assumed isenthalpic expansion [25] can be either in the gaseous or two-phase region. As shown in Figure 4, helium expands in the gaseous state in the case of Exp. 1 while for Exp. 2 the two-phase region is reached. However, the sizing of the SRV has been carried out with the gaseous K_{dr} for both experiments, validated two-phase K_{dr} values for helium are not available. [16] suggests to use the gaseous K_{dr} whenever the flow is choked as it is in both experiments. Further investigations will be carried out to study the influence of two-phase flow and to test correlations for two-phase discharge coefficients.

5. Conclusion and outlook

Based on first experimental results, the PICARD instrumentation was successfully upgraded with a lift sensor and two pressure transmitters. Further experiments have been conducted.

The results validate the calculation of the deposited heat flux and show that due to the dynamic process, the heat flux relevant for sizing is lower than the commonly assumed values. Furthermore, the significance of the fluid state on the sizing was demonstrated. In particular the influence of two phase flow on the discharge coefficient.

Therefore, further investigations both on the heat flux and the discharge coefficient will be carried out. Experiments with different SRVs under variation of set pressure and filling level are planned in the frame of the R&D collaboration between KIT and CERN. As part of this collaboration, all experimental results will be implemented in a future version of CERN Kryolize® software [26], a reference calculation program for sizing of SRD.

6. References

[1] DIN EN ISO 4126 2013 Safety devices for protection against excessive pressure – Part 7: Common data., German version
[2] API Standard 520 2014 Sizing, selection, and installation of pressure-relieving devices
[3] Cavallari G, Gorine I, Güsewell D and Stierlin R 1989 *4th Workshop on RF Superconductivity Japan* 781–803
[4] Lehmann W and Zahn G 1978 *IPC Business Press* 569–579
[5] Harisson S 2001 *IEEE Transactions on Applied Superconductivity* 1343–1346
[6] Heidt C 2017 *Experimental Investigation and Modelling of Incidents in Liquid Helium Cryostats* Unp. thesis Karlsruhe Institute of Technology Karlsruhe
[7] Heidt C, Henriques A, Stamm M and Grohmann S 2016 *IOP Conference Series: Materials Science and Engineering* ISSN 1757-8981
[8] Heidt C, Schön H, Stamm M and Grohmann S 2015 *IOP Conference Series: Materials Science and Engineering* **101** 012161 ISSN 1757-8981
[9] Datskov V I and Weisend J G 1994 *Cryogenics Vol 34 ICEC supplement*
[10] Grohmann S and Süßer M 2013 *Proceedings of CEC-ICMC*
[11] DIN EN ISO 21013 2016 Cryogenic vessels – pressure-relief accessories for cryogenic service - Part 3: Sizing and capacity determination. German version
[12] Varghese A and Zhang B 1992 *Advances in Cryogenic Engineering Materials* 1487–1492
[13] Leung J C 2004 *Journal of Loss Prevention in the Process Industries* **17** 301–313 ISSN 09504230
[14] Lenzing T, Friedel L, Cremers J and Alhusein M 1998 *Journal of Loss Prevention in the Process Industries* **11** 307–321 ISSN 09504230
[15] Sallet D W 1984 *Nuclear Science and Engineering* 220–244
[16] Darby R 2004 *Journal of Loss Prevention in the Process Industries* **17** 255–259 ISSN 09504230
[17] Lemmon E W, Huber M L and McLinden M O 2013 Refprop, reference fluid thermodynamic and transport properties. Version 9.1
[18] Wagner W and Pru A 2002 *Journal of Physical and Chemical Reference Data* **31** 387–535 ISSN 0047-2689
[19] Tegeler C, Span R and Wagner W 1999 *Journal of Physical and Chemical Reference Data* **28** 779–850 ISSN 0047-2689
[20] Schmidt R and Wagner W 1985 *Fluid Phase Equilibria* **19** 175–200 ISSN 03783812
[21] Bäcker D and Wagner W 2006 *Journal of Physical and Chemical Reference Data* **35** 205–266 ISSN 0047-2689
[22] DIN EN ISO 5167 2004 Measurement of fluid flow by means of pressure differential devices inserted in circular cross-section conduits running full – Part 4: Venturi tubes. German version
[23] Bureau International des Poids et Mesures 2008 Evaluation of measurement data – guide to the expression of uncertainty in measurement
[24] European Parliament 2014 Pressure equipement directive 2014/68/eu
[25] DIN SPEC 4683 2015 Cryostats for liquefied helium – safety devices for protection against excessive pressure.
[26] Henriques A 2015 KT fund application for Kryolize project CERN EDMS N. 155418

Acknowledgments

The authors would like to acknowledge the support from the CERN Knowledge Transfer Group and the KIT Legal Department in the process of finalizing the R&D collaboration agreement. The authors would also like to acknowledge the support from the Karlsruhe School of Elementary Particle and Astroparticle Physics: Science and Technology (KSETA).